Acta Crystallographica Section D
Biological Crystallography
ISSN 0907-4449

Structural adaptation of endonuclease I from the cold-adapted and halophilic bacterium *Vibrio salmonicida*

Bjørn Altermark,[a] Ronny Helland,[a] Elin Moe,[a] Nils P. Willassen[a,b] and Arne O. Smalås[a]*

[a]Norwegian Structural Biology Centre, Faculty of Science, University of Tromsø, N-9037 Tromsø, Norway, and [b]Department of Molecular Biotechnology, Faculty of Medicine, University of Tromsø, N-9037 Tromsø, Norway

Correspondence e-mail: arne.smalas@chem.uit.no

Received 3 October 2007
Accepted 2 January 2008

PDB Reference: *V. salmonicida* endonuclease I, 2pu3, r2pu3sf.

The crystal structure of the periplasmic/extracellular endonuclease I from *Vibrio salmonicida* has been solved to 1.5 Å resolution and, in comparison to the corresponding endonucleases from *V. cholerae* and *V. vulnificus*, serves as a model system for the investigation of the structural determinants involved in the temperature and NaCl adaptation of this enzyme class. The overall fold of the three enzymes is essentially similar, but the *V. salmonicida* endonuclease displays a significantly more positive surface potential than the other two enzymes owing to the presence of ten more Lys residues. However, if the optimum salt concentrations for the *V. salmonicida* and *V. cholerae* enzymes are taken into consideration in the electrostatic surface-potential calculation, the potentials of the two enzymes become surprisingly similar. The higher number of basic residues in the *V. salmonicida* protein is therefore likely to be a result, at least in part, of adaptation to the more saline habitat of *V. salmonicida* (seawater) than *V. cholerae* (brackish water). The hydrophobic core of all three enzymes is almost identical, but the *V. salmonicida* endonuclease has a slightly lower number of internal hydrogen bonds. This, together with repulsive forces between the basic residues on the protein surface of *V. salmonicida* endonuclease I and differences in the distribution of salt bridges, probably results in higher flexibility of regions of the *V. salmonicida* protein. This is likely to influence both the catalytic activity and the stability of the protein.

1. Introduction

Cold adaptation of enzymes has often been shown to invoke structural changes that lead to lower thermal stability and increased catalytic efficiency in comparison with mesophilic orthologues. These two properties are believed to be common to all cold-adapted enzymes (Feller & Gerday, 1997). Much research has been undertaken in order to determine how this is achieved. There seem to be many ways in which an enzyme can change during evolution in response to low temperature and each enzyme class is probably unique in its adaptation strategy (Smalås *et al.*, 2000). One theory states that in order to increase the catalytic efficiency at low temperatures the enzymes increase their flexibility, which is in turn responsible for the observed lower temperature stability (Hochachka & Somero, 1984). The increase in flexibility is hard to prove experimentally, but the theory is generally accepted on the basis of calorimetric data, molecular-dynamics simulations, comparison of X-ray structures, hydrogen–deuterium

exchange rates and other indirect measurements of flexibility. Adaptation of thermophilic enzymes shows the opposite trend with respect to stability and catalytic efficiency when compared with mesophilic and psychrophilic orthologues. It seems that enzymes adapt by optimizing their flexibility at their physiological temperatures. The increase in flexibility of cold-adapted enzymes is not easily detectable by comparing X-ray structures because of the marginal energy of stabilization that all enzymes display. However, a decrease in the number of hydrogen bonds, salt bridges and hydrophobic interactions are thought to be involved in the increase in flexibility. Larger surface-loop areas and optimized electrostatic interactions in and around the active site have also been reported (Russell, 2000).

Salinity is another physical parameter that enzymes must adapt to. Compositional studies of proteins from halophiles show a statistical increase in negatively charged amino acids (Oren *et al.*, 2005). This increase in acidity is thought to prevent aggregation (Elcock & McCammon, 1998). Seawater at 3.5% salinity contains about 470 m*M* Na^+ and 540 m*M* Cl^- (Turekian, 1968). Most marine prokaryotes can therefore be characterized as slight halophiles (Oren, 2000) and their periplasmic/extracellular proteins are exposed to the full salinity of the environment. In order to obtain further information on the mechanisms involved in both temperature and NaCl adaptation of enzymes, we have focused on the elucidation of the structure of endonuclease I from the psychrophilic and marine bacterium *Vibrio salmonicida* (*Vs*EndA). This enzyme and the orthologous mesophilic enzyme from the brackish water bacterium *V. cholerae* (*Vc*EndA) have previously been characterized biochemically (Altermark, Niiranen *et al.*, 2007); the structure of *Vc*EndA is also known from previous work (Altermark *et al.*, 2006). *Vs*EndA shows typical cold-adapted properties such as lower temperature stability, higher catalytic efficiency and lower temperature optimum for activity when compared with *Vc*EndA. The catalytic efficiency of the cold-adapted enzyme is optimized through an increase in k_{cat}. The K_m is slightly higher compared with that of *Vc*EndA. *Vs*EndA is also more NaCl-dependent than *Vc*EndA (Altermark, Niiranen *et al.*, 2007). In addition, a third structure from the marine mesophilic *V. vulnificus* is available both in its native form and in complex with an 8 bp and a 16 bp dsDNA oligomer (Li *et al.*, 2003; Wang *et al.*, 2007). The catalytic mechanism has also been outlined (Li *et al.*, 2003), in which His80 functions as a general base which activates a water molecule for an in-line attack on the scissile phosphate. The Mg^{2+} ion stabilizes the transition state and an Mg^{2+}-bound water molecule provides a proton to the 3′-oxygen leaving group. Arg99 is thought to stabilize the product *via* a hydrogen bond to the scissile phosphate group. The Mg^{2+}-coordinating amino acids lie in a conserved $\beta\beta\alpha$-metal fold present in many nucleases. A statistical study of cold and salt adaptation of endonuclease I sequences has also been published (Altermark, Thorvaldsen *et al.*, 2007). The main conclusions were that the surface isoelectric point and surface hydrophobicity increased in the cold-adapted sequence population but decreased in the salt-adapted sequence population. However, an increase in isoelectric point was found to be a cold- and salt-adaptive trend when considering the active-site region of the enzyme. The structures, statistical analysis and biochemical data provide a good platform for the elucidation of the mechanisms behind temperature and NaCl adaptation of endonuclease I from *V. salmonicida*.

2. Materials and methods

2.1. Crystallization

The gene encoding EndA from *V. salmonicida* was cloned, recombinantly produced in *Escherichia coli* and purified as described previously (Altermark, Niiranen *et al.*, 2007). Initial screening of crystallization conditions was conducted using Hampton Crystal Screens I and II. Crystals of *Vs*EndA were obtained using the hanging-drop vapour-diffusion technique at room temperature. All drops were generated by mixing 1.0 µl enzyme solution (dissolved in 20 m*M* Tris buffer pH 8.3, 10 m*M* $MgSO_4$ and approximately 0.4 *M* NaCl) with 1.0 µl precipitant solution on siliconized cover slides and were equilibrated against 1.0 ml of the same precipitant solution.

2.2. Data collection and structure determination

Crystals were soaked in mother liquor containing 15%(*w*/*v*) glycerol prior to flash-cooling in liquid nitrogen. X-ray intensity data were collected from a single crystal on ID29 of the European Synchrotron Radiation Facility (ESRF), Grenoble, France. Intensity data were collected using a CCD detector at a wavelength of 1.0707 Å and with a crystal-to-detector distance of 115 mm. 200 images were collected using an oscillation of 1.0°. The data were processed using *MOSFLM* (Powell, 1999), *SCALA* and *TRUNCATE* in the *CCP*4 program suite (Collaborative Computational Project, Number 4, 1994). The structure was solved by molecular replacement with *MOLREP* (Vagin & Teplyakov, 1997) in *CCP*4 using the substrate-free structure of *V. vulnificus* endonuclease (PDB code 1ouo; Li *et al.*, 2003) as a search model. The structure was built using a combination of autobuilding in *ARP*/*wARP* (Perrakis *et al.*, 1999) and manual refitting of side chains using *O* (Jones *et al.*, 1991) based on σ_A-weighted $2mF_o - DF_c$ and $mF_o - DF_c$ electron-density maps. Refinement was carried out in *REFMAC*5 (Murshudov *et al.*, 1999) from the *CCP*4 suite. The model was validated using *PROCHECK* (Laskowski *et al.*, 1993) and *WHATCHECK* (Hooft *et al.*, 1996).

2.3. Structural comparison

The structural alignment was created using the *EsPript* web server (Gouet *et al.*, 1999). *LSQKAB* from the *CCP*4 program package (Collaborative Computational Project, Number 4, 1994) were used to calculate the r.m.s.d. between the main-chain atoms of the three enzymes. Amino-acid sequences were analyzed using the aliphatic index (Ikai, 1980) and the instability index (Guruprasad *et al.*, 1990). The PDB codes are 1ouo (native) and 1oup (active-site mutant in complex with an 8 bp DNA oligomer) for *V. vulnificus* endonuclease I (Vvn)

Table 1
Data-collection and refinement statistics for *Vs*EndA.

Values in parentheses are for the outer shell (1.58–1.50 Å).

Data collection	
Resolution limit, edge (Å)	1.5
Unit-cell parameters (Å, °)	a = 42.08, b = 44.95, c = 51.75, β = 92.66
Space group	$P2_1$
Wavelength (Å)	1.0707
Total no. of reflections	123750
No. of unique reflections	30823
Completeness (%)	99.3 (97.6)
$I/\sigma(I)$	9.4 (8.4)
R_{merge} (%)	4.7 (7.4)
Multiplicity	4.0 (3.7)
Wilson B (Å^2)	10.24
Refinement	
R_{work} (%)	16.26
R_{free} (%)	18.27
Average B factor (Å^2)	10.45
No. of protein atoms	1702
No. of solvent molecules (including ions)	271
R.m.s. deviations	
Bond lengths (Å)	0.006
Bond angles (°)	1.039
Ramachandran plot (%)	
Most favoured	91.9
Additionally allowed	7.6
Generously allowed	0.5
Disallowed	0

and 2g7e for *Vc*EndA. Salt bridges were calculated using the *WHAT IF* web server (Rodriguez *et al.*, 1998). The *VADAR* v.1.4 server (Willard *et al.*, 2003) was used for the calculation of the water-accessible surface areas and hydrogen bonds. Only the first amino-acid conformation was used with both the *VADAR* and the *WHAT IF* servers. Amino acids at the N- or C-terminus that were not present in electron density in all structures were disregarded in the calculations. Electrostatic surface potentials were calculated using *DelPhi* (Rocchia *et al.*, 2001) and visualized using the *PyMOL* program (DeLano, 2002). H atoms were added before the calculation and the internal and external dielectric constants were set to 4 and 80, respectively. Atomic partial charges were taken from the molecular-simulation program *AMBER* (Case *et al.*, 2005). Potentials were calculated both at the optimum NaCl concentration (*Vc*EndA, 175 m*M*; *Vs*EndA, 425 m*M*) and without NaCl. The electrostatic surface potentials of DNA taken from the Vvn structure in complex with a dsDNA octamer were also calculated at the same NaCl concentration as for the enzymes.

3. Results

3.1. Crystallization, data collection, structure determination and refinement

Thin plate-like crystals of *Vs*EndA grew within a few days from 30% PEG 3350, 0.1 *M* Tris pH 8.2 and 0.25 *M* sodium acetate. The crystal diffracted to beyond 1.25 Å, but data could not be collected to higher resolution owing to restrictions in the crystal-to-detector distance. Data were therefore integrated to 1.5 Å (the edge of the detector) and data-collection and refinement statistics are listed in Table 1. The crystal belonged to space group $P2_1$, with one molecule in the asymmetric unit.

MOLREP found one clear rotation solution with a rotation function/σ value of 14.03 that was 9.2σ better than the second best solution. The R factor and correlation coefficient after translation searches were 45.5% and 42.6%, respectively. Parts of the structure were poorly defined in electron density in the initial maps. These were therefore rebuilt by autobuilding using *ARP*/*wARP* in combination with manual refitting of side chains and loops based on $2mF_o - DF_c$ and $mF_o - DF_c$ electron-density maps. The final structure includes 1973 atoms including one magnesium ion, two chloride ions and 268 water molecules; R_{work} and R_{free} were 16.60% and 18.50%, respectively.

The electron density is in general well defined for the structure, as shown in Fig. 1(*a*), except at the termini. The first four residues are not defined at all in the structure and only parts of the two last residues could be fitted into electron density. Residues with poorly defined side chains include those belonging to or close to the DNA-binding sites (*e.g.* residues 26, 69, 70, 96 and 156) or crystal contact regions (residues 69, 70, 96, 156, 198, 211 and 226). All residues with poor electron density, with the exceptions of Gln69, Glu70 and Glu211, are Lys or Arg residues in structural proximity. These are likely to repel each other because of insufficient stabilization of the positive potential of the side

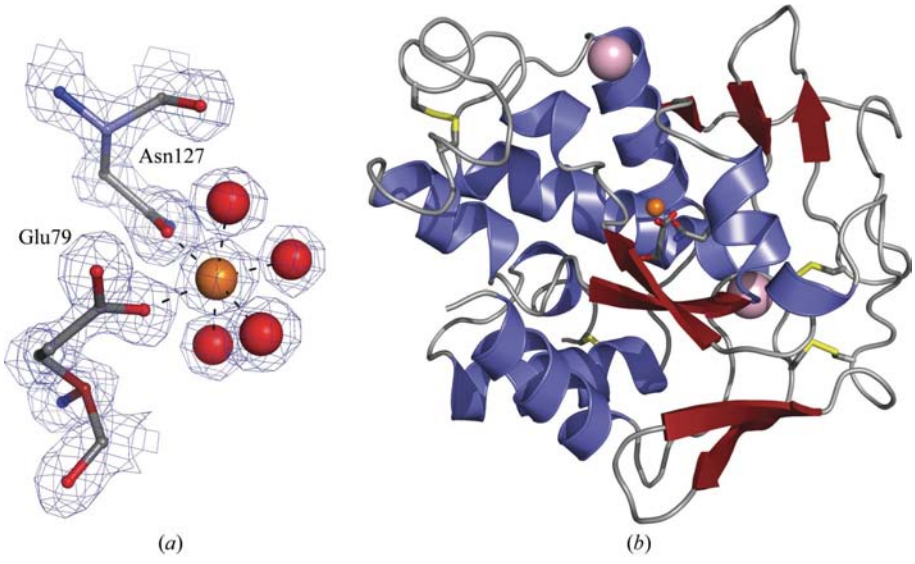

Figure 1
(*a*) Electron-density map ($2mF_o - DF_c$) contoured at 1.7σ showing the magnesium ion in orange and the coordinating amino acids Glu79, Asn127 and four water molecules in an octahedral geometry around the magnesium ion. (*b*) Ribbon representation of *V. salmonicida* endonuclease I. Pink and orange spheres represent chloride and magnesium ions, respectively.

chain by negatively charged residues or solvent molecules. This will be discussed further below.

Magnesium and chloride ions were found to be present at positions identical to those in the *Vc*EndA and Vvn structures and with similar distances to the coordinating atoms. In addition, a second chloride ion was found on the surface of *Vs*EndA (Fig. 1*a*) which coordinates to the conserved residues Gln86, Ser186 and Gln189 in addition to two water molecules.

3.2. Structural comparison to VcEndA and Vvn

*Vs*EndA shares 71 and 73% sequence identity with the endonucleases from *V. cholerae* and *V. vulnificus*, respectively (Fig. 2).

The fold of the three structures is practically identical and *Vs*EndA superimposes on *Vc*EndA and Vvn with r.m.s.d. values of 0.87 and 0.91 Å, respectively, for main-chain atoms. The differences observed are generally in regions involved in crystal packing. The *Vs*EndA structure deviates slightly from the two other enzymes in three regions (Trp50–Gly55, Ser141–Phe145 and Tyr181–Ser186) as shown in Fig. 3.

The difference in the orientation in the first region is caused by the insertion of a Lys after residue 52 in *Vs*EndA (Lys52a). The two other regions form crystal contacts with each other and it is therefore difficult to determine whether the differences are real or a result of the crystal packing. In *Vs*EndA Lys52a is close to the DNA-binding site as defined for the Vvn structure (PDB code 1oup; Li *et al.*, 2003) and may potentially have an effect on catalysis. The two other regions are farther away from the DNA-binding site and are therefore not expected to affect substrate binding significantly.

Table 2
Number of salt bridges and hydrogen bonds, theoretical isoelectric point, number of positive and negative amino acids, ratio of large/(large + small) hydrophobic residues, aliphatic index, instability index and percentage sequence identity to *Vs*EndA.

The sequence identity between *Vc*EndA and Vvn is 73%.

	*Vs*EndA	*Vc*EndA	Vvn
Salt bridges < 6 Å	50	53	53
Salt bridges < 4 Å	21	22	21
Total hydrogen bonds	235	245	241
pI	9.6	8.6	9.0
(Arg + Lys + His)	41	31	33
(Asp + Glu)	20	22	20
(Leu + Ile)/(Leu + Ile + Val + Ala)	0.36	0.40	0.41
Aliphatic index	49.06	54.08	49.91
Instability index	45.87	39.32	45.03
Identity to *Vs*EndA (%)	—	71	73

An investigation of surface properties and sequence statistics is presented in Table 2.

There is a large increase in the number of positively charged amino acids in *Vs*EndA, resulting in a very high theoretical pI. This is primarily caused by the presence of a higher number of Lys residues in *Vs*EndA. *Vs*EndA also has a slightly higher number of Ala residues than the other two enzymes. This increase in Lys and Ala content seems to be at the expense of Asn and Gln residues (a total of 28 in *Vs*EndA, 35 in *Vc*EndA and 37 in Vvn). The number of hydrogen bonds is lower in

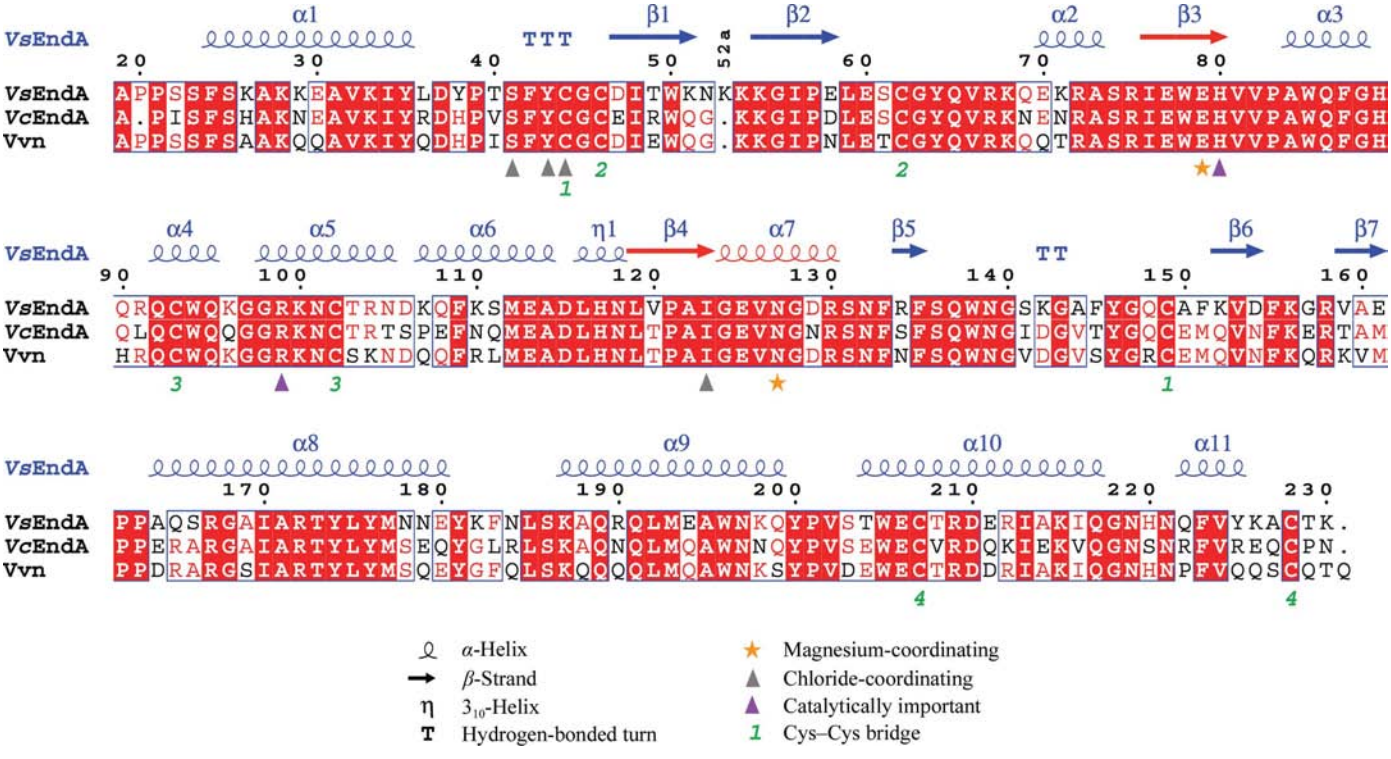

Figure 2
Structural alignment based on the secondary structure of *Vs*EndA. The $\beta\beta\alpha$-metal fold is marked with secondary-structure elements in red. The amino-acid numbering is according to the Vvn structure.

*Vs*EndA than in the other two enzymes (Table 2), but the number of interactions between O and N atoms shorter than 4.0 Å in residues forming salt bridges (including His) is similar in the three structures. *Vs*EndA and *Vc*EndA have three salt-bridge networks involving three residues, while Vvn has one such network. Five salt bridges are conserved in all three structures (Asp37–Arg212/Lys212, Glu77–Arg72, Glu79–Arg130, Glu113–Arg99 and Asp206–Arg172). Asp210 is involved in the three-residue network in all three structures, forming one interaction to His117 in all structures and a second interaction to Arg225 in *Vc*EndA and His220 in *Vs*EndA and Vvn. Asp37 forms a salt bridge to residue 212 in all three structures. This residue is Lys in *Vc*EndA and Arg in *Vs*EndA and Vvn. Two of the salt bridges (Asp129–Arg67 and Asp154–Lys142) found in *Vs*EndA but not in *Vc*EndA are in the vicinity of the DNA-binding site (Fig. 4). When investigating an alignment created in a previous study (Altermark, Thorvaldsen *et al.*, 2007), we found that Arg67 is totally

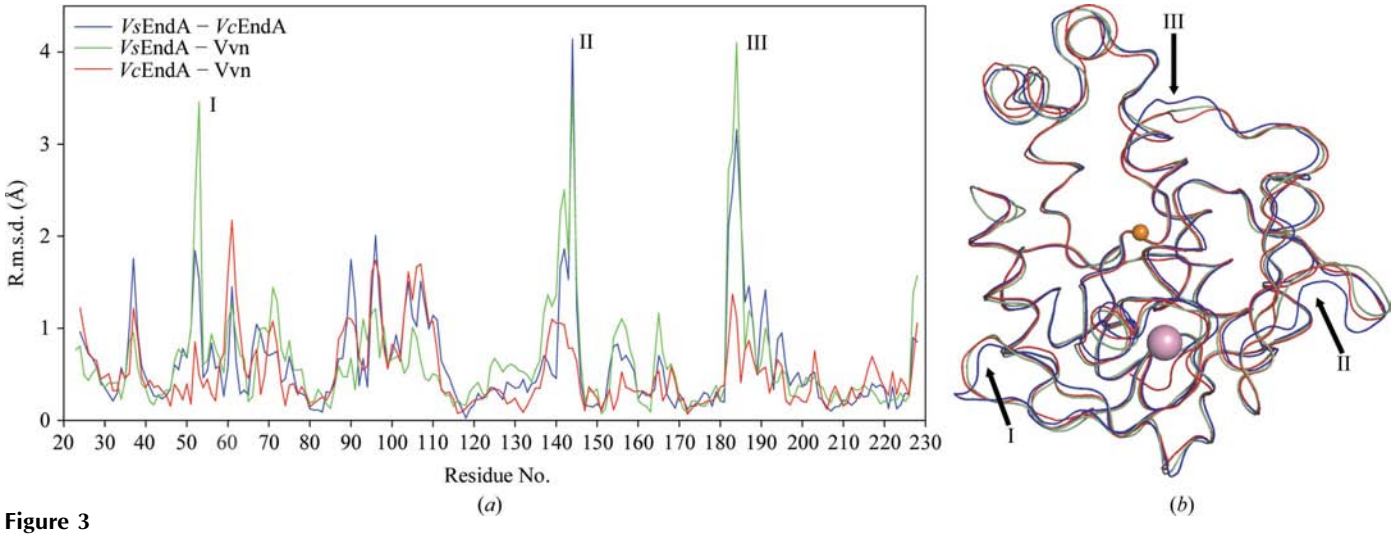

Figure 3
(*a*) Main-chain r.m.s.d.s between *Vs*EndA and *Vc*EndA (blue), *Vs*EndA and Vvn (green) and *Vc*EndA and Vvn (Guruprasad *et al.*, 1990). (*b*) Backbone traces of *Vs*EndA (blue), *Vc*EndA (Guruprasad *et al.*, 1990) and Vvn (green). The arrows indicate areas in which the r.m.s.d. of *Vs*EndA is particulary high compared with the other two structures. Roman numerals are added to facilitate comparison between the figures.

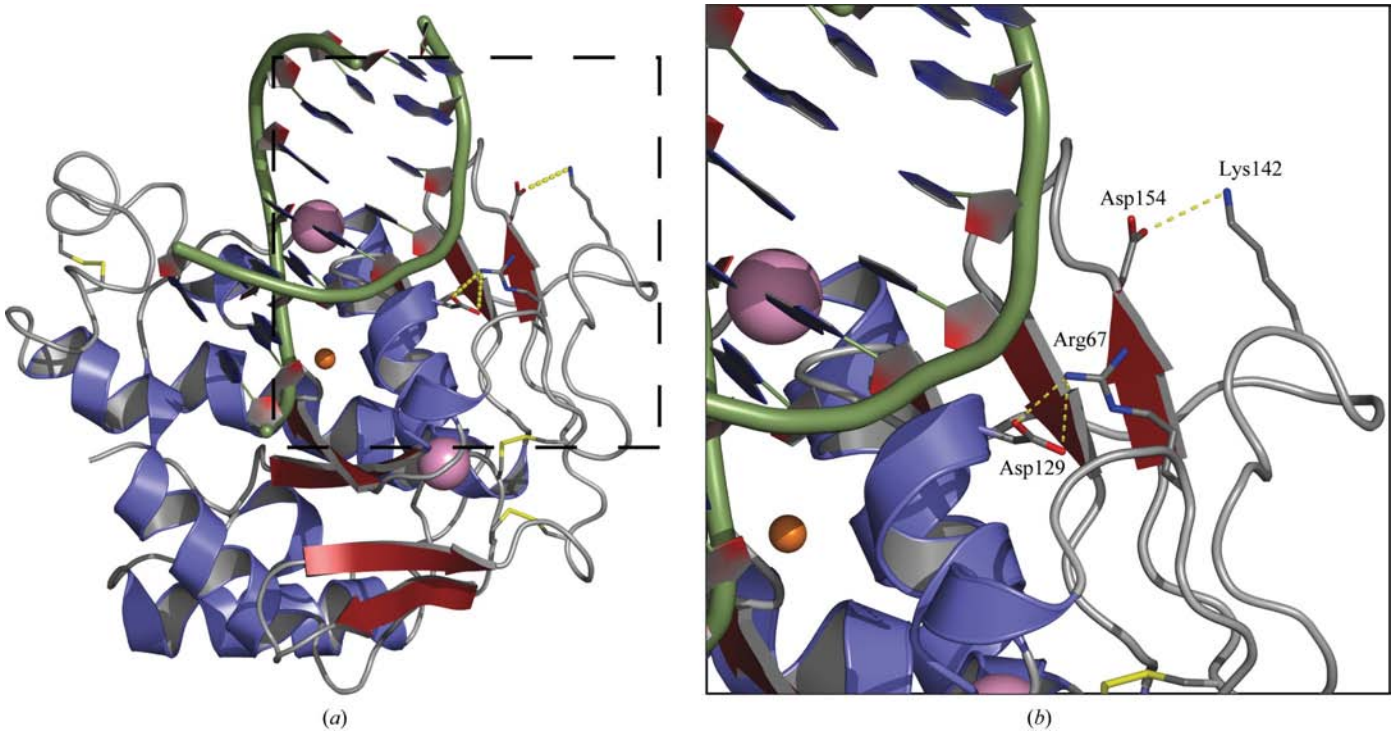

Figure 4
Two salt bridges present close to the DNA-binding site in *Vs*EndA (Asp129–Arg67 and Asp154–Lys142) but not in *Vc*EndA. The DNA from the Vvn–DNA structure is illustrated as a green ladder. The pink and orange spheres are chloride and magnesium ions, respectively. (*a*) Overall structure, (*b*) close up of area marked in (*a*).

conserved and Asp129 is also highly conserved. However, among the strains of *V. cholerae* versions of the sequence exist with an Asn at position 129 like the one we have studied. It is likely that the absence of this conserved salt bridge will affect the properties of *Vc*EndA.

Three salt bridges are found at the C-terminus of *Vc*EndA (Glu179–Arg222, Glu214–Arg225 and Glu226–Arg222; Fig. 5). These are unique to this enzyme and are also found to be unique when comparing against other EndA sequences from the *Vibrionaceae* family present in GenBank.

The instability index and aliphatic index (Table 2) both indicate that *Vs*EndA is a less stable enzyme than *Vc*EndA and Vvn.

Electrostatic surface potentials of *Vc*EndA and *Vs*EndA, calculated without NaCl and at the NaCl concentration for optimal activity, are shown in Fig. 6.

The positive surface potentials of both enzymes are reduced in buffer that includes NaCl and the two enzymes apparently have an almost equal surface potential surrounding the DNA-binding site at their respective salt optima for activity. As shown in Figs. 6(*e*), 6(*f*) and 6(*g*), the negatively charged phosphate backbone of DNA is also influenced by NaCl and becomes more neutral with increasing NaCl concentration.

4. Discussion

The kinetic behaviour of *Vs*EndA and *Vc*EndA has previously been characterized (Altermark, Niiranen *et al.*, 2007). The results showed that at temperatures of 278, 288, 298, 303 and 310 K *Vs*EndA possessed a higher k_{cat} than *Vc*EndA and its K_m was slightly higher. These measurements were performed in optimal buffer for each enzyme (75 m*M* diethanolamine pH 8.5, 5 m*M* $MgCl_2$, 425 m*M* NaCl for *Vs*EndA and 75 m*M* diethanolamine pH 8.0, 5 m*M* $MgCl_2$, 175 m*M* NaCl for *Vc*EndA). The catalytic efficiency at 310 K was in the 10^8 s^{-1} M^{-1} range for both enzymes, making them almost perfect catalysts (Stroppolo *et al.*, 2001). The environment in which *Vs*EndA and *Vc*EndA are meant to function seems to correlate well with the different optimal buffers for activity. Vvn is not well characterized, but the relatively high theoretical pI of the enzyme (Table 2) and the intermediate NaCl optimum for growth of the bacterium (Strom & Paranjpye, 2000) may indicate that Vvn is also highly activated by NaCl.

The structural explanations for the observed differences in K_m, k_{cat}, optimum salt concentration and stability between *Vs*EndA and *Vc*EndA are not in all cases obvious. The fold of the two proteins is almost identical, with a sequence identity of about 71%. However, the differences in the distribution of amino acids and salt bridges on the enzyme surfaces may explain the differing behaviour of the enzymes.

4.1. Adaptation to NaCl

*Vs*EndA appears to have adapted to higher NaCl concentrations by increasing the number of positively charged residues on the enzyme surface. These residues are distributed all over the surface, but with a slight clustering on the side facing the DNA substrate. A lower salt concentration than the optimal 425 m*M* may result in an affinity for the substrate that

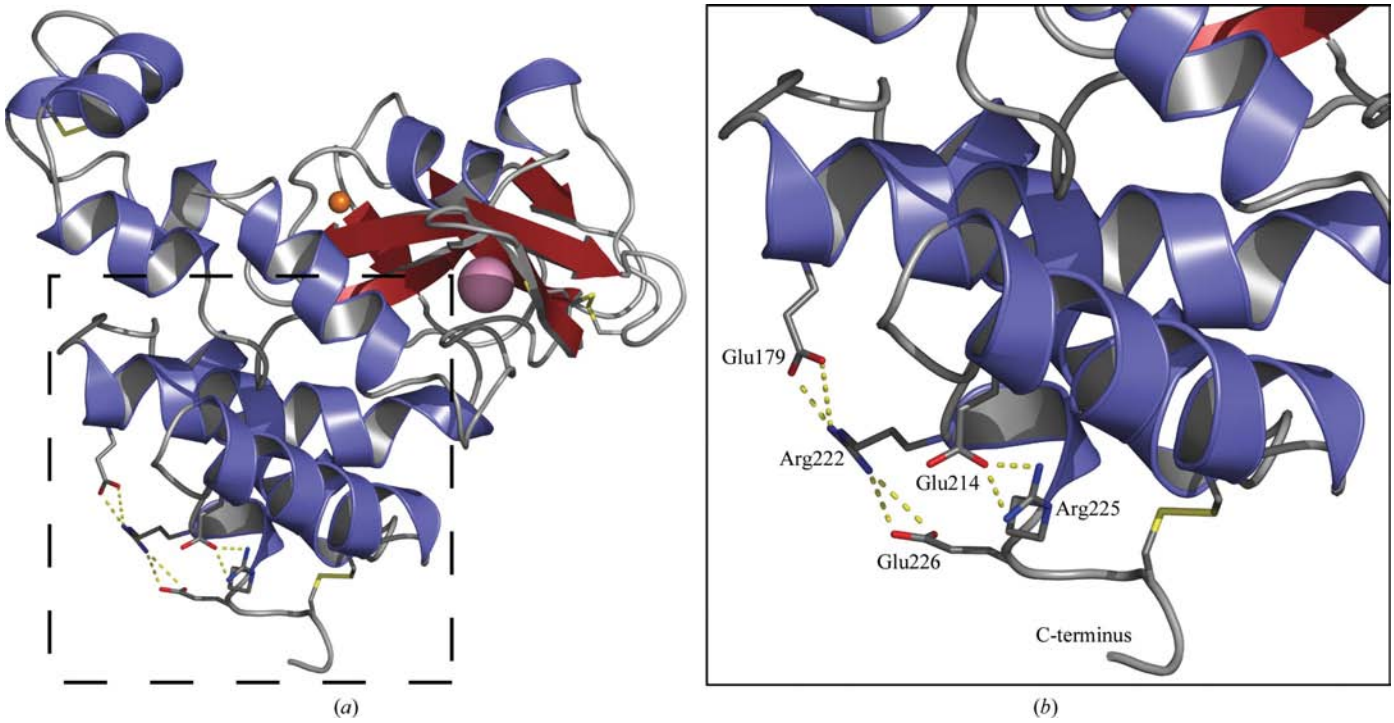

Figure 5
Three salt bridges (Glu179–Arg222, Glu214–Arg225 and Glu226–Arg222) present close to the C-terminus of the structure in *Vc*EndA but not in *Vs*EndA. The pink and orange spheres are chloride and magnesium ions, respectively. (*a*) Overall structure, (*b*) close up of area marked in (*a*).

is too strong for efficient catalysis and release of the product. It should be noted that the concentration of NaCl also influences the electrostatic potential of the substrate. Therefore, the optimal activity of the two enzymes has to involve a fine-tuning of reduction of the positive potentials of the enzyme-binding sites and the negative potential of the DNA substrate.

In addition to the conserved buried chloride ion that is present in all three structures, *Vs*EndA also contains a surface chloride ion. This chloride ion coordinates to conserved residues and is therefore likely to be a result of the different crystallization conditions rather than a specific chloride-binding site.

4.2. Stability and flexibility

Increased catalytic efficiency of psychrophilic enzymes is generally accepted to be caused by an increase in the flexibility of the protein, primarily owing to looser core packing and fewer hydrogen bonds and salt bridges. The hydrophobic core of the three structures is not very different as judged by structural comparison of internal residues. Therefore, the interactions that result in differences in biophysical properties are expected to essentially be caused by residues on the enzyme surfaces. The much larger number of lysine residues in *Vs*EndA does not seem to cause an increase in the number of protein hydrogen bonds or an increase in the number of salt bridges that could potentially result in a less flexible structure. In contrast, the *V. salmonicida* endonuclease has fewer hydrogen bonds than *Vc*EndA and Vvn and this is in accordance with the theory of cold adaptation. The number of salt bridges <6 Å in length is slightly lower in *Vs*EndA compared with both *Vc*EndA and Vvn, but the number of strong salt bridges (<4 Å) is almost equal. At high salt concentrations the charged residues of the endonucleases are likely to form interactions with the ions. The strength of the salt bridges will be reduced on increasing the NaCl concentration because of Debye–Huckel screening of the electrostatic interactions. It is therefore reasonable to believe that the salt bridges stabilize the *Vs*EndA structure somewhat less than the *Vc*EndA structure. The highly cationic character of *Vs*EndA (pI 9.6), with an increase of ten positively charged residues, also indicates the presence of a destabilizing electrostatic repulsion between the positive charges that makes the enzyme less stable and more flexible. However, such repulsive forces may be weakened by NaCl (Nishimura *et al.*, 2001). Unique repulsive forces in *Vs*EndA appear to be present between residues Lys26, Lys29, Lys33 and Lys53. The side chains of the amino acids in the 51–54 (KNKKK) loop of *Vs*EndA lack electron density,

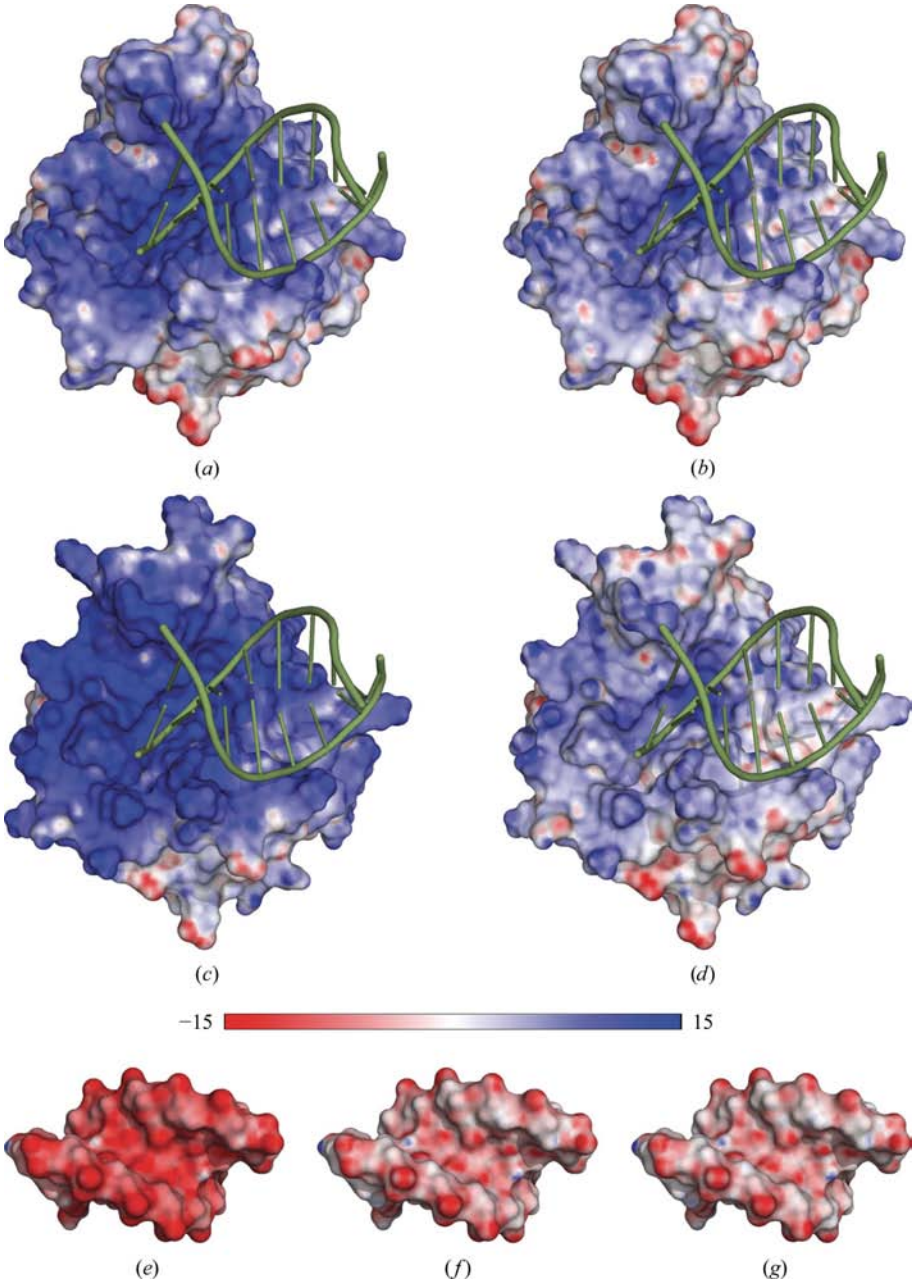

Figure 6
Electrostatic surface potential of *Vc*EndA, *Vs*EndA and a DNA oligomer. (*a*) *Vc*EndA without NaCl and (*b*) with 175 m*M* NaCl. (*c*) *Vs*EndA without NaCl and (*d*) with 425 m*M* NaCl. The DNA ribbon shown in green is superimposed from the structure of Vvn in complex with a DNA octamer (PDB code 1oup). (*e*) DNA without NaCl, (*f*) with 175 m*M* NaCl and (*g*) with 425 m*M* NaCl. The orientation of the DNA is as in (*a*)–(*d*), except that it is rotated 180° around the *x* axis to visualize the side facing the enzyme. The electrostatic potential between $-15k_BT/e$ and $15k_BT/e$ is indicated as a colour gradient from red to blue.

something that may be indicative of repulsive forces acting between those residues. Another interesting region of the *Vs*EndA structure, which is close to the DNA-binding site and which is not conserved, is residues 69–71 (QEK). Lys71 is 6.4 Å from one of the O atoms of the phosphate group in DNA as determined by superimposing the *Vs*EndA structure onto the Vvn–DNA complex. This lysine may be important for improving the physiological efficiency of *Vs*EndA by optimizing the orientation of the enzyme's active site to face the negatively charged DNA. The higher K_m for *Vs*EndA compared with *Vc*EndA at all temperatures may indicate that *Vs*EndA is more flexible and that this flexibility decreases the substrate binding, as hypothesized by Fields (2001).

Four salt bridges are unique to *Vc*EndA, of which three are located in the C-terminal region (Fig. 5). *Vc*EndA has a 8 K higher calorimetric T_m than *Vs*EndA (Altermark, Niiranen *et al.*, 2007). It is reasonable to believe that the salt bridges, which prevent the unfolding of the C-terminus upon heating, can cause some of the increased stability.

4.3. Affinity for substrate

A greater number of positively charged residues at or close to the active site should in principle favour binding of the negatively charged DNA. Kinetic analysis has previously shown that K_m for *Vs*EndA and *Vc*EndA is relatively similar at the temperatures analyzed if the NaCl concentration for optimum activity is used (Altermark, Niiranen *et al.*, 2007). If we make the assumption that K_m is indicative of substrate affinity, it is clear that *Vs*EndA does not have higher substrate affinity. The electrostatic surface potentials of *Vs*EndA and *Vc*EndA (Fig. 6), calculated at their respective NaCl optima, reveal that the two enzymes have an almost equally charged surface. This suggests that the salt reduces some of the positive surface potential of VsEndA owing to Debye–Huckel screening of the charges. NaCl is also known to stabilize the double-stranded conformation of DNA (Clausen-Schaumann *et al.*, 2000). The phosphate groups are screened by Na^+ and the negative charges that repel each other are weaker in a buffer containing NaCl, as shown in Figs. 6(*e*), 6(*f*) and 6(*g*). The net effect of NaCl on both the DNA and the enzyme seems therefore to be tightly linked to the affinity between the substrate and enzyme.

Surface epitopes particularly rich in Arg and Lys residues appear to have higher flexibility in *Vs*EndA than in *Vc*EndA, according to the electron-density maps. Increased flexibility at the substrate-binding site may prove unfavourable as efficient substrate binding may be weaker. However, some of the flexibility may be slightly reduced by the introduction of the salt bridges 67–129 and 142–154 in *Vs*EndA (Fig. 4) and 72–77–75 in all three structures. It is also possible that the stabilizing effect of these salt bridges disappears at high salt concentration since the K_m for *Vs*EndA is higher than *Vc*EndA at the salt optimum. The fact that the 67–129 salt bridge is missing in *Vc*EndA (but is present in other strains of *V. cholerae*) could be an indication of a less important function of the salt bridge in this enzyme, especially since *V. cholerae* is a less salt-adapted species.

5. Conclusion

In this paper, we have reported the crystal structure of an endonuclease from the psychrophilic *V. salmonicida*. The structure has been solved to 1.5 Å and has been compared with those of the homologous enzymes from *V. cholerae* and *V. vulnificus*. The fold of the three enzymes is essentially identical and the major difference is the much greater number of lysine residues in the *Vs*EndA structure. The increased number of lysines does not seem to increase the number of hydrogen bonds or salt bridges, but the resulting increase in electrostatic surface potential is significant and as an isolated effect would have had a great impact on the physical properties of the enzyme. However, the electrostatic surface potentials calculated at the respective NaCl optima of *Vs*EndA and *Vc*EndA display remarkable similarity around the substrate-binding site.

The greater number of lysine residues in *Vs*EndA seems to serve two adaptational purposes. On one hand, *Vs*EndA has had to adapt to low temperature. An increased positive surface potential would favour the binding of a negatively charged substrate, but too tight binding may prevent release of the product. Higher flexibility of the enzyme is desired in order to perform efficient catalysis at low temperatures and this appears to be accomplished, among other methods, by placing several positively charged residues relatively close together in three-dimensional space such that the region(s) becomes destabilized. On the other hand, the enzyme has to adapt to the salinity of the habitat. NaCl can screen the electrostatic surface potential of both the enzyme and substrate. It is therefore reasonable to believe that the increase in lysine content in *Vs*EndA is not solely a result of adaptation to the low temperature of its natural habitat, but is also a result of the necessity to adapt to the salinity of the habitat. The ratio of lysine content *versus* NaCl concentration is therefore probably a fine-tuned compromise between the need to increase the substrate affinity and the need to destabilize the protein to obtain sufficient flexibility for efficient catalysis in a cold saline environment. Site-directed mutagenesis is being pursued in order to assess the significance of the observed structural differences between *Vs*EndA and *Vc*EndA.

The present study was supported by the National Functional Genomics Program (FUGE) of The Research Council of Norway and by Biotec Pharmacon ASA. Provision of beamtime at the macromolecular beamlines at the European Synchrotron Radiation Facility (ESRF) is gratefully acknowledged.

References

Altermark, B., Niiranen, L., Willassen, N. P., Smalås, A. O. & Moe, E. (2007). *FEBS J.* **274**, 252–263.

Altermark, B., Smalås, A. O., Willassen, N. P. & Helland, R. (2006). *Acta Cryst.* D**62**, 1387–1391.
Altermark, B., Thorvaldsen, S., Moe, E., Smalås, A. O. & Willassen, N. P. (2007). *Comp. Biol. Chem.* **31**, 163–172.
Case, D. A., Cheatham, T. E. III, Darden, T., Gohlke, H., Luo, R., Merz, K. M. Jr, Onufriev, A., Simmerling, C., Wang, B. & Woods, R. J. (2005). *J. Comput. Chem.* **26**, 1668–1688.
Clausen-Schaumann, H., Rief, M., Tolksdorf, C. & Gaub, H. E. (2000). *Biophys. J.* **78**, 1997–2007.
Collaborative Computational Project, Number 4 (1994). *Acta Cryst.* D**50**, 760–763.
DeLano, W. L. (2002). *PyMOL*. DeLano Scientific, San Carlos, USA. http://www.pymol.org.
Elcock, A. H. & McCammon, J. A. (1998). *J. Mol. Biol.* **280**, 731–748.
Feller, G. & Gerday, C. (1997). *Cell. Mol. Life Sci.* **53**, 830–841.
Fields, P. A. (2001). *Comp. Biochem. Physiol. A*, **129**, 417–431.
Gouet, P., Courcelle, E., Stuart, D. I. & Metoz, F. (1999). *Bioinformatics*, **15**, 305–308.
Guruprasad, K., Reddy, B. V. & Pandit, M. W. (1990). *Protein Eng.* **4**, 155–161.
Hochachka, P. W. & Somero, G. N. (1984). *Biochemical Adaptation.* Princeton, USA: Princeton University Press.
Hooft, R. W., Vriend, G., Sander, C. & Abola, E. E. (1996). *Nature (London)*, **381**, 272.
Ikai, A. (1980). *J. Biochem. (Tokyo)*, **88**, 1895–1898.
Jones, T. A., Zou, J.-Y., Cowan, S. W. & Kjeldgaard, M. (1991). *Acta Cryst.* A**47**, 110–119.
Laskowski, R. A., Moss, D. S. & Thornton, J. M. (1993). *J. Mol. Biol.* **231**, 1049–1067.
Li, C. L., Hor, L. I., Chang, Z. F., Tsai, L. C., Yang, W. Z. & Yuan, H. S. (2003). *EMBO J.* **22**, 4014–4025.
Murshudov, G. N., Vagin, A. A., Lebedev, A., Wilson, K. S. & Dodson, E. J. (1999). *Acta Cryst.* D**55**, 247–255.
Nishimura, C., Uversky, V. N. & Fink, A. L. (2001). *Biochemistry*, **40**, 2113–2128.
Oren, A. (2000). *The Prokaryotes*, Vol. 2, edited by M. Dworkin, S. Falkow, E. Rosenberg, K.-H. Schleifer & E. Stackebrandt, pp. 263–282. New York, USA: Springer.
Oren, A., Larimer, F., Richardson, P., Lapidus, A. & Csonka, L. N. (2005). *Extremophiles*, **9**, 275–279.
Perrakis, A., Morris, R. & Lamzin, V. S. (1999). *Nature Struct. Biol.* **6**, 458–463.
Powell, H. R. (1999). *Acta Cryst.* D**55**, 1690–1695.
Rocchia, W., Alexov, E. & Honig, B. (2001). *J. Phys. Chem. B*, **105**, 6507–6514.
Rodriguez, R., Chinea, G., Lopez, N., Pons, T. & Vriend, G. (1998). *Bioinformatics*, **14**, 523–528.
Russell, N. J. (2000). *Extremophiles*, **4**, 83–90.
Smalås, A. O., Leiros, H. K., Os, V. & Willassen, N. P. (2000). *Biotechnol. Annu. Rev.* **6**, 1–57.
Strom, M. S. & Paranjpye, R. N. (2000). *Microbes Infect.* **2**, 177–188.
Stroppolo, M. E., Falconi, M., Caccuri, A. M. & Desideri, A. (2001). *Cell. Mol. Life. Sci.* **58**, 1451–1460.
Turekian, K. K. (1968). *Oceans.* Englewood Cliffs, USA: Prentice–Hall.
Vagin, A. & Teplyakov, A. (1997). *J. Appl. Cryst.* **30**, 1022–1025.
Wang, Y. T., Yang, W. J., Li, C. L., Doudeva, L. G. & Yuan, H. S. (2007). *Nucleic Acids Res.* **35**, 584–594.
Willard, L., Ranjan, A., Zhang, H., Monzavi, H., Boyko, R. F., Sykes, B. D. & Wishart, D. S. (2003). *Nucleic Acids Res.* **31**, 3316–3319.